

EXPLORING VOLATILE DEPOSITION IN LUNAR REGOLITH. J.A. Alford¹, A.R. Hodges¹, E. Heggy² and A.P.S. Crotts¹, ¹Columbia University, Columbia Astrophysics Laboratory, New York, NY 10027; arh2156, jaa2168, apc5@columbia.edu; ²Jet Propulsion Laboratory, Radar Science Group, Pasadena, CA 91109; heggy@jpl.nasa.gov

Introduction: Various and reinforcing evidence indicates volatiles trapped in the lunar regolith near the North and South Poles. Epithermal neutron absorption betrays the presence of hydrogen, presumably water, deep in permanently shadowed regions (PSRs), and in regions far from PSR [1,2,3]. This indicates hydrogen at depths to 1 meter or more, although in places covered by a desiccated layer. Radar observations, particularly circular polarization return, also indicate water to similarly shallow depths [4]. The excavation of regolith by *LCROSS* showed a large part of the regolith's mass made of volatiles, perhaps increasing with depth, to at least 3 meters [5,6]. Migration of volatiles depositing out of the vacuum is limited to the first meter in depth, but can be impact-gardened into regolith a meter deeper or more [7]. Conversely if water vapor percolates through regolith via outgassing from the lunar interior (as seen from fire fountains about 3.5 Gy ago [8]), it is also capable of freezing in the regolith, especially in polar regions but not necessarily in PSRs [9]. This might explain hydrogen in regolith detected via epithermal neutron absorption far from PSRs.

We present preliminary results from two studies useful in understanding these processes: 1) we ask at what depths, depending on local topography, surface-deposited volatiles will be buried as a function of time not only by impact gardening, but by secular increase in regolith depth due to erosion of nearby terrain (as expected for depressions amid impact-eroded high points); and 2) we examine ground-penetrating radar data from regolith in regions of hydrogen-containing PSRs, in non-PSR hydrogen-rich areas, and in nearby control areas in to understand how hydration interacts with the regolith. This is a work in progress; further results will be presented at the meeting.

Impact Gardening versus Secular Deposition Rates for Regolith in Varying Terrain:

We will present at the meeting the asymmetric deposition of ejecta on slopes representative of large crater walls, as derived from a numerical N-body simulation of impacts using Newtonian ballistics and empirical ejecta values. These show significant rates of regolith deposition on the floors below crater walls, at a level comparable to or exceeding local impact gardening rates.

Radar Analysis of Regions with Depressed Epithermal Neutron Flux: For radar data from Mars, we were able to successfully probe for subsurface ice using MARSIS data after accounting for surface rough-

ness over the site. [10] We are employing an identical technique here for candidate hydrated area on the Moon.

The Lunar Exploration Neutron Detector (LEND) instrument onboard the *Lunar Reconnaissance Orbiter* spacecraft detected regions of elevated epithermal neutron flux, indicating the presence of hydrogen, near the lunar poles. We perform a follow-up investigation of one of these regions, which is not permanently shadowed from the Sun. Radar data from the Lunar Radar Sounder (LRS) instrument onboard the *SELENE* spacecraft is analyzed to investigate the presence of water ice in this region.

We selected a site within the hydrogen enriched region and a control site outside the hydrogen enriched region that have similar smooth topography. The coordinates of these sites are at (Lat, Long) = (85.5, 133.6) and (86.9, 133.1), respectively. The topography of the sites along the Selene track, measured by the Lunar Orbiter Laser Altimeter (LOLA), is plotted in Figure 1. Since the sites have similar smooth topography, differences in radar attenuation indicate differences in the dielectric constant of the regolith.

The Selene radargram is shown in Figure 3. The hydrogen rich site is marked on the left and the control site is marked on the right. We took the average attenuation profile of 11 consecutive pixels (corresponding to 840m) along the *SELENE* track at both the hydrogen rich site and the control site. (see Figure 2) These attenuation profiles are normalized at the lunar surface. The decreased attenuation rate in the hydrogen rich site is consistent with the dielectric properties of water ice-rich material. [10] Hydrogen enrichment is correlated with the observed radar loss rate, which are lower for hydrogen-rich areas. This is in the same sense that has been found from the Mars MARSIS subsurface ice and for terrestrial results.

References:

- [1] Feldman W. C. et al. (1998) *Science*, 281, 1496. [2] Mitrofanov I.G. et al. (2010) *Science*, 330, 483. [3] Sanin A. et al. (2010) *Lunar Exploration & Analysis Group Meeting*: (<http://www.lpi.usra.edu/meetings/leag2010/presentations/WedAM/saninEtAl.pdf>). [4] Spudis P. D. et al. (2010) *GRL*, 37, L06204. [5] Colaprete A. et al. (2010) *Science*, 330, 463. [6] Colaprete A. et al. (2011) in "A Wet vs. Dry Moon" LPI, 2011 June 13-16, #6011. [7] Grieves G. et al. (2010) *LPSC LXI*, 2552. [8] Saal A. et al. (2008) *Nature*, 454, 192.

[9] Crofts A.P.S. & Hummels C. (2009) *ApJ*, 707, 1506. [10] Boisson J. et al. (2009) *JGRE*, 114, E08003.

(horizontal), and the vertical scale from the bottom to the surface is 6 km.

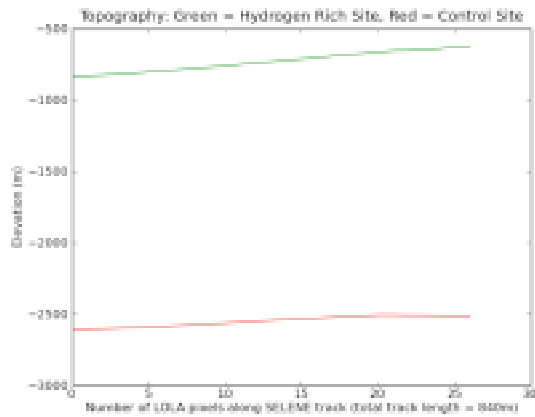


Figure 1: The elevation of the hydrogen rich site (green curve) and control (red curve) over 840 meters track length in each case, as measured by LRO/LOLA, as an indication of surface roughness, which is smooth in both cases.

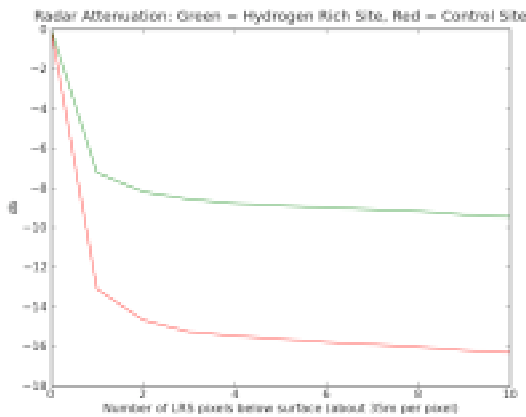


Figure 2: The attenuation (in decibels) normalized with zero at the surface, for the hydrogen rich (green) and control (red) sites. The uppermost layers are much less lossy (by about 6 db). This can be interpreted as consistent with the behavior of water ice.

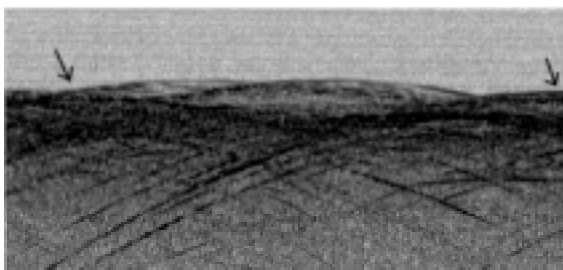


Figure 3: The radargram from SELENE/LRS of both the hydrogen-rich site (left arrow) and control (right arrow). The distance between the arrows is 41 km